A BALANCED CASCADE 26-40GHz AMPLIFIER

D.M.F. McCANN

Marconi Electronic Devices Ltd
Doddington Road, Lincoln, LN6 3LF ENGLAND

ABSTRACT

This paper described the design, fabrication and performance of a balanced cascade 26-40GHz amplifier. The circuit is fabricated using an advanced multilayer thin film technology on a glass ceramic substrate material. Details and results for the quadrature coupler design, termination approach and amplifier technique will be presented.

INTRODUCTION

In recent years a number of people have reported their work on 26-40GHz amps using both HEMT's and MESFET's [1], [2], [3]. These reports have largely placed their emphasis on the semi-conductor device technology. This paper will present an improved amplifier design through advances in substrate technology, semi-monolithic processing techniques and component design. The practical result is a 26-40GHz amplifier in balanced form offering 9.0dB minimum gain, input and output VSWR <2.0:1 and noise figure <6.0dB.

SEMICONDUCTOR DEVICE

The selection of high performance mm-wave devices from the few commercially available was based on the results of in-house characterisation data up to 26GHz. Two MESFET devices were selected, referred to as MESFET #1 and #2, gate periphery 0.25μm x 200 and 0.25 x 65 μm, respectively. An investigation of available HEMT's deemed the MESFET structure more applicable, from a reliability and power handling capability, for the EW application anticipated.

DIELECTRIC MEDIUM

Quartz and Alumina tend to form the base for most thin film circuits used at mm-wave frequencies. A new glass ceramic material, dielectric constant 5.8, developed at GEC Ceramics was used in the design of this amplifier. This material is easily profiled and lasered and its low porosity and fine grain nature lends itself to fine line patterning because of the smooth surface finish which is attainable. Compromising the dielectric constant value between Quartz and Alumina results in both an improved aspect ratio and reduced conductor losses in the coupler, whilst limiting proximity effects in the balanced amplifier.

CIRCUIT FABRICATION

A new thin film technology which allows the integration of capacitors, resistors and air-bridge interconnections has been developed. Initially intended for use with Alumina substrates it is called MICROWAVE MONOLITHIC ALUMINA CIRCUIT (MiMAC) processing. Further recent developments have lead to the use of MiMAC technology on a variety of substrate materials using both dielectric and conducting media. Fig. 1 shows a flow diagram illustrating the processing sequence used to fabricate the multilayer thin film circuit.

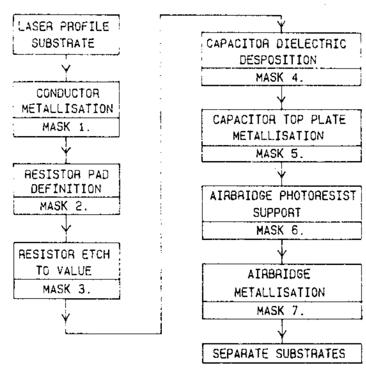

FIGURE 1. PROCESS FLOW DIAGRAM

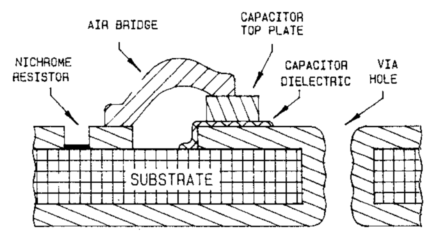

FIGURE 2. DEFINED MiMAC CROSS-SECTION

The balanced amplifiers were fabricated on 0.254mm thick, laser profiled glass ceramic substrate material. An automatic sputtering machine is used to deposit the nichrome/gold conductor metallisation. Pattern plating defines the conductor pattern whilst integrated resistors and resistive films are defined by selective plasma etching. Parallel plate integrated MIM capacitors

CH2725-0/89/0000-0845$01.00 © 1989 IEEE

are formed from a layer of silicon nitride which is deposited using a PECVD process. All cross-over and capacitor top-plate interconnections are made using air-bridges. A profile of an advanced MiMAC circuit is show in Fig. 2.

COUPLER DESIGN

The 3dB hybrid coupler was based on a variant of the interdigitated Lange coupler (4), see Fig. 3. Initial line width and spacings were obtained theoretically, however, optimisation of the coupler match, insertion loss, coupling and phase balance was undertaken using "4 times" modelling techniques. Using this approach considerable improvements were obtained in the match and insertion loss at the upper end of the frequency band. The resulting line widths and spacings and their realisation on the lower dielectric material proved complementary given the benefits of reduced losses, better aspect ratio and improved

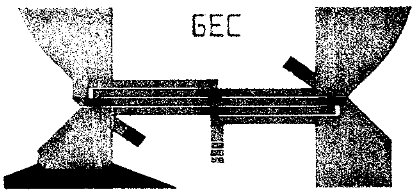

FIGURE 3. INTERDIGITATED LANGE COUPLER

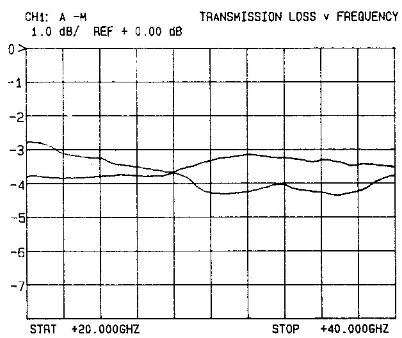

FIGURE 4. THROUGH AND COUPLED PORT PERFORMANCE

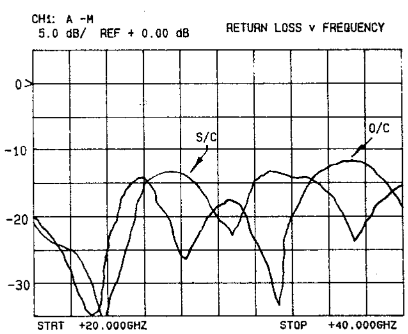

FIGURE 5. COUPLER RETURN LOSS UNDER MISMATCH CONDITIONS

fabrication accuracy. Fig. 4 shows the resulting through and coupled port performance whilst Fig. 5 shows the match under open and short circuit conditions.

TERMINATION DESIGN

The role played by the termination load, traditionally a 50 ohm resistor to ground, is to absorb the reflected energy in a balanced component design where mismatching occurs. However, distributed effects, due to the finite length of the resistor and its path to ground, result in the load becoming more reflective with increasing frequency, Fig. 6(a). The new termination described here does not use a 50 ohm lumped resistor nor does it have a path to ground. Reflected energy is dissipated in a distributed planar load fabricated in a thin film resistive material. Scale modelling of the layout and variation of the ohms/square in the resistive material resulted in the compact planar load shown in Fig. 7. Fig 6(b) shows the resulting return loss.

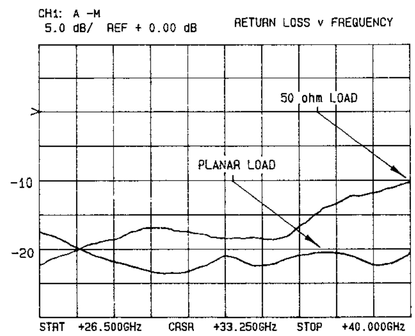

FIGURE 6. MEASURED RETURN LOSS RESULTS . (a) 50 ohm LOAD . (b) PLANAR LOAD

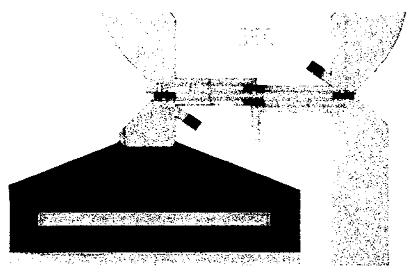

FIGURE 7. DISTRIBUTED PLANAR LOAD

AMPLIFIER DESIGN AND PERFORMANCE

In designing the 26-40GHz Amplifier the S-parameters have been calculated up to 40GHz by an equivalent circuit analysis using measured s-parameters over 2-26.5GHz. Initially, optimised single ended designs utilising standard lossless reactive matching techniques were developed, and combined using the hybrid coupler and planar load detailed earlier to form balanced amplifiers. Fig 8 and Fig. 9 show the single ended and balanced results which were obtained.

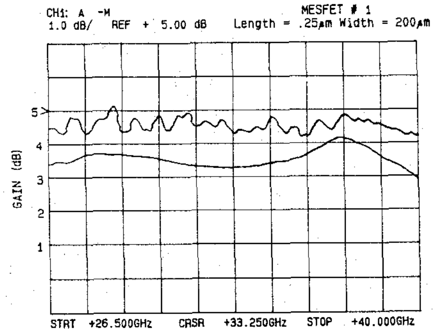

FIGURE 8. MEASURED SINGLE-ENDED AND BALANCED RESULTS . MESFET # 1

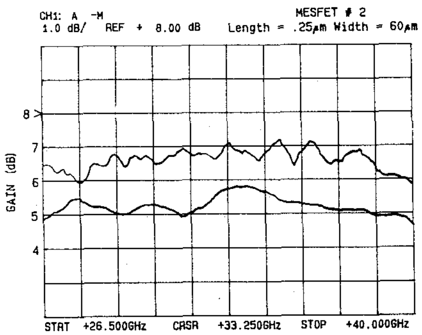

FIGURE 9. MEASURED SINGLE-ENDED AND BALANCED RESULTS . MESFET # 2

Further investigation using synthesis and optimisation tools revealed the possibility of combining two devices in cascade, whilst maintaining stable performance, optimum gain and minimum gain flatness. Self biassing was used throughout and the bias paths for the gate and drain lines were included in the matching topologies. In particular, the addition of a shunt gate grounding inductance also serves to ensure the unconditional stability of the device at lower frequencies. A stability analysis of the interstage network and the effect of balancing confirms the overall stability of the cascade. Fig. 11 shows the single-ended equivalent circuit which forms half of the balanced design, known as the Balanced Cascade. The degree of isolation

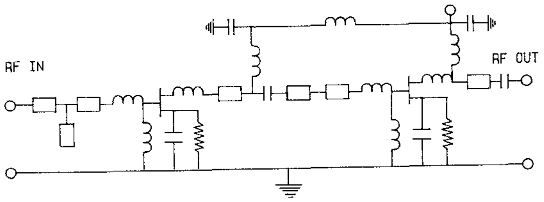

FIGURE 10. SINGLE ENDED CASCADE EQUIVALENT CIRCUIT

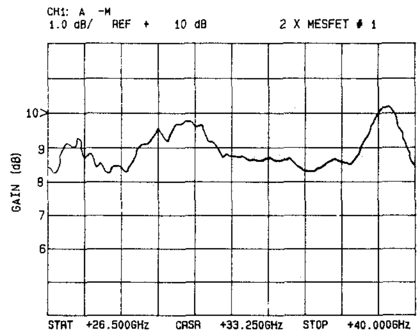

FIGURE 11. MEASURED RESULTS SINGLE-ENDED CASCADE . TYPE (1)

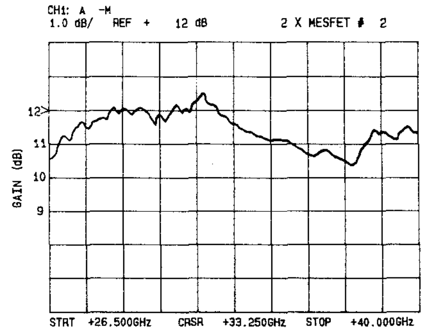

FIGURE 12. MEASURED RESULTS SINGLE-ENDED CASCADE . TYPE (2)

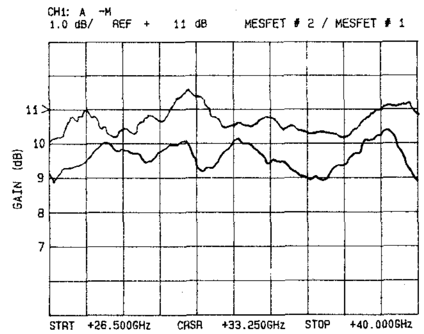

FIGURE 13. MEASURED SINGLE-ENDED AND BALANCED CASCADE RESULTS . TYPE (3)

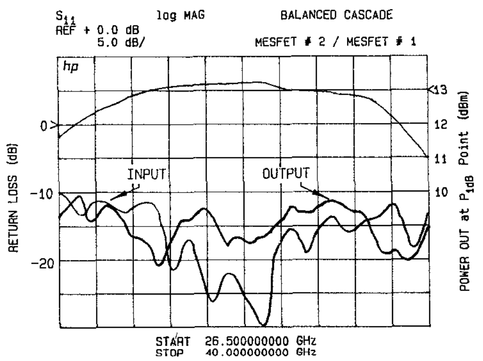

FIGURE 14. MEASURED RETURN LOSS AND COMPRESSION RESULTS . TYPE (3)

provided by the coupler and planar load, when subject to the mismatch conditions detailed previously in Fig. 5, allow the stage to be tuned for gain and gain flatness without concern for reflected power. The versatility and success of this approach are reflected in the measured results detailed in Figs. 11,12,13 and 14. Results show that the Balanced Cascade offers two major advances over a standard balanced amplifier, 1) a reduced second stage noise contribution and 2) the corresponding increase in length is less than 40% whilst gain is more than doubled resulting in the highest gain per unit length reported to date.

AMPLIFIER CONSTRUCTION

The various components making up the balanced amplifiers were fabricated using MiMAC techniques. The completed substrates are attached to lipped interconnecting titanium carriers. The application of lipped carriers eases the problem of maintaining a continuous ground in the amplifier chain and reduces the earth return path at the module interface. To prevent waveguide moding at the high end of the operating frequency range, the cavity in which the stages are installed must be sufficiently small enough in width and height, thus the finished sizes of the standard balanced amplifier and balanced cascade are 3.25 x 5.9mm and 3.25 x 8.2mm respectively. In this small size the circuit layout, whilst ensuring r.f. performance, must also maximise the isolation between r.f. circuitry and d.c. lines. Fig. 15 shows a single stage MiMAC 26-40GHz Balanced Cascade amplifier, whilst Fig. 16 shows the application of the 26-40GHz amplifier in a temperature compensated Ka-Band frequency converter.

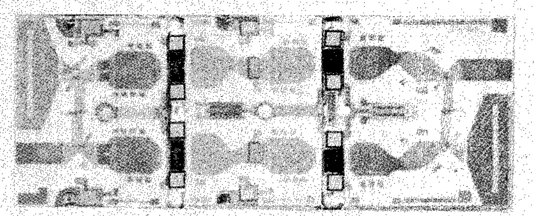

FIGURE 15. SINGLE STAGE MiMAC 26-40 GHz BALANCED CASCADE AMPLIFIER

CONCLUSION

Through the use of novel design techniques in the field of amplifier design, coupler design termination design and semi-monolithic thin-film processing, a balanced cascade 26-40GHz amplifier has been developed. Gain >9.0dB, Noise figure <6.0dB, VSWR <2.0:1 and P_{1dB} >11dBm represent the best results reported for a unit Ka-Band MIC amplifier to date. Reduced fixed assembly costs, reduced parasitics, improved reliability and repeatable performance represent the potential advantages of semi-monolithic component design at mm-wave frequencies. This represents a significant step forward in the production engineering of mm-wave microstrip designs. Application of these technology advances in a Ka-Band EW frequency converter unit has proven very effective in achieving balanced temperature compensated modules with higher gain.

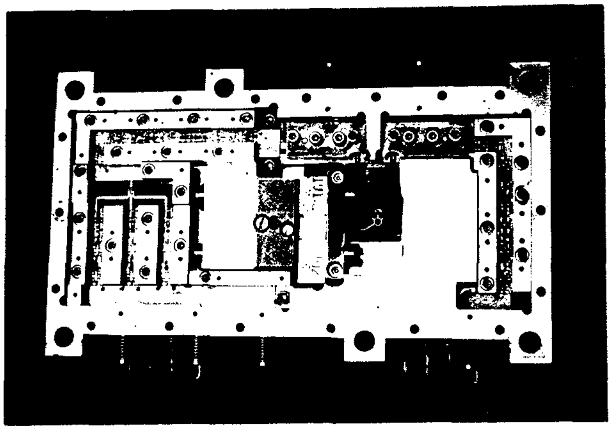

FIGURE 16. TEMPERATURE COMPENSATED Ka-BAND FREQUENCY CONVERTER

ACKNOWLEDGEMENT

The author would like to make special acknowledgement to Mr. P. Blunden for his contributions to this work.

REFERENCES

(1) K. Shabita, et. al "Broadband HEMT Amplifier for 26.5-40.0GHz, 1987 IEEE MTT-S Digest,p.1011.

(2) J. Roenberg, et al, "A 26.5-40.0GHz GaAs FET Amplifier", 1982 IEEE MTT-S Digest, p.166-168.

(3) K. Shabita, et al, "Broadband HEMT and GaAs FET Amplifiers for 18-26.5GHz", 1985 IEEE MTT-S Digest, p.547-550.

(4) Y. Tajima, Susumu Kamihashi "Multiconductor Couplers", IEEE Trans. Microwave Theory Tech., Vol. MTT-26, P795, 1978.